Frequency Diverse Array Focusing Beampattern Synthesis With Constrained Nonlinear Programming Frequency Offsets

Yan-Shuo Cui, Hui Chen, *Member, IEEE*, Wen-Qin Wang, *Senior Member, IEEE*

***Abstract*— Different phased-array only providing angle-dependent array factor, frequency diverse array (FDA) offers both angle- and range-dependent array factor. In this letter, we optimally design FDA frequency offsets by formulating a constrained nonlinear programming problem to produce range-angle focusing beampattern. The corresponding time-variance characteristics of the optimized FDA beampattern are also analyzed. The proposed method is verified by simulation results, which superiority to existing Log-FDA, Hamming-FDA and GA-FDA methods are validated.**

***Index Terms*—Frequency diverse array (FDA), constrained nonlinear problem, time-variance, beampattern synthesis, beampattern focusing.**

I. Introduction

FREQUENCY diverse array (FDA) technology [1]–[4] is a new direction to provide joint space (*i.e.,* angle and range) focusing in the future. Unlike traditional phased-array (PA) that only synthesizes angle-dependent beampattern, the beampattern generated by FDA also depends on the range [5]. In [6], a frequency diverse chirp waveform structure was used to generate range-angle coupled beampattern together with the ambiguity analysis. In [7], full-wave analysis of FDA was studied with the finite difference time domain method.

As FDA has inherent range dependence that PA does not have, FDA has many potential applications such as target parameter estimation [8], [9], microwave imaging [10]–[12], RF stealth [13] and so on. However, the standard FDA will produce range and angle coupled beampattern [14], which is a disadvantage in parameter estimation [15]. To generate uncoupled range-angle beampattern for FDA, there are two ways to choose: 1) uniform frequency offsets and nonuniform element spacing [16], 2) uniform element spacing and nonuniform frequency offsets. Since nonuniform element spacing is not easy to change in real time according to the actual needs, it is necessary to focus the beampattern.

Dai *et al.* [17], [18] adopted a multi-carrier FDA geometry and convex optimization to achieve uncoupled range-angle beampattern. Khan *et al.* [19] used logarithmic frequency offsets to decouple the range-angle beampattern, but the beampattern has serious power leakage and poor resolution that will degrade its parameter estimation performance. In [14], symmetrical frequency offsets and Hamming windowing were involved to generate a focusing beampattern at the cost of high sidelobes. In addition, genetic algorithm (GA) was used [20] to search for a set of nonlinear frequency offsets for a focusing beampattern, but the GA requires high computational complexity. In [21]–[23], time-modulated frequency offsets were adopted to producing time-invariant beampattern within a time duration, but the beampattern is in fact still time variant.

In this letter, we optimally design the frequency offsets by solving a constrained nonlinear optimization problem to generate a range-angle focusing beampattern, which achieves superior resolution to existing Log-FDA [19], Hamming-FDA [14] and GA-FDA [20] schemes. Furthermore, time-variance of the FDA beampattern is also analyzed. The remainder of this letter is organized as follows. The proposed FDA focusing beampattern synthesis is presented in Section II, and simulation results and discussions are given in Section III. Finally, conclusions are drawn in Section IV.

II. FDA Focusing Beampattern Synthesis

Consider a linear FDA with M elements spaced by $d = \lambda/2$ with λ being the wavelength. The radiated frequency of the m-th element is

$$f_m = f_0 + \Delta f_m,\ m = 0, 1, \ldots, M-1 \tag{1}$$

where f_0 and Δf_m denote the carrier frequency and nonlinear frequency offset for the mth element, respectively. The continuous-time signal transmitted by the mth element can be expressed as

$$x_m(t) = w_m \exp(j2\pi f_m t),\ t \in [0, T] \tag{2}$$

where w_m is the corresponding complex weight, and T is the signal duration.

Taking the first element as the reference, for an arbitrary far-field position with angle θ and range r, the radiation distance for the mth element can be approximated by $r_m \approx r - md\sin\theta$. The overall transmitted signals can then be expressed as

$$\begin{aligned} x(t; r, \theta) = &\exp\left\{j2\pi f_0\left(t - \frac{r}{c_0}\right)\right\} \sum_{m=0}^{M-1} w_m \exp\{j2\pi\Delta f_m t\} \\ &\times \exp\left\{-j2\pi\frac{\Delta f_m r - f_0 md\sin\theta - m\Delta f_m d\sin\theta}{c_0}\right\} \end{aligned} \tag{3}$$

where c_0 is the speed of light. Note that, since $f_0 md\sin\theta/c_0 \gg m\Delta f_m d\sin\theta/c_0$, the last term $m\Delta f_m d\sin\theta/c_0$ is neglectable.

This work was supported in part by the National Natural Science Foundation of China (61501089, 61571081), Sichuan Science and Technology Program (18ZDYF2551, 2018RZ0141), and Fundamental Research Funds for the Central Universities (ZYGX2018J005).

The authors are with School of Communication and Information Engineering, University of Electronic Science and Technology of China, Chengdu, P. R. China (email: 201621010415@std.uestc.edu.cn; huichen0929@uestc.edu.cn; wqwang@uestc.edu.cn).

978-9-0827-9703-9/19/$31.00 ©2019 IEEE

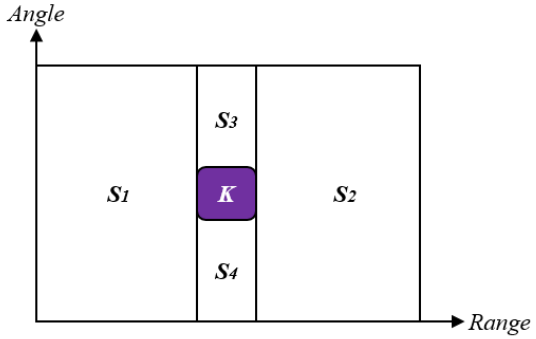

Fig. 1: Two-Dimensional mapping of main beam region and sidelobe regions.

The corresponding array factor (AF) is

$$\begin{aligned}\mathrm{AF}(t;r,\theta) \approx & \sum_{m=0}^{M-1} w_m \exp(j2\pi\Delta f_m t) \\ & \times \exp\left\{-j2\pi\frac{(\Delta f_m r - f_0 m d\sin\theta)}{c_0}\right\}\end{aligned} \tag{4}$$

According to (4), it is worth noticing that:

1) Given the angle $\theta = \theta_k$ for $\forall t \in [0, T]$, the quasi-static beampattern is affected by both range r and frequency offset Δf_m.

2) Given range $r = r_k$ for $\forall t \in [0, T]$, the quasi-static beampattern is only related to angle θ.

For notational convenience, we rewrite (4) as

$$AF(t;r,\theta) = \mathbf{w}^T \mathbf{a}(t;r,\theta) \tag{5}$$

where ^{T} is the transpose operator. To steer the beampattern to the target position (r_k, θ_k), the weight vector $\mathbf{w}$ should be

$$\mathbf{w} = \begin{bmatrix} \exp\left\{-j2\pi\frac{\Delta f_0 r_k}{c_0}\right\} \\ \exp\left\{-j2\pi\frac{\Delta f_1 r_k - f_0 d\sin\theta_k}{c_0}\right\} \\ \vdots \\ \exp\left\{-j2\pi\frac{\Delta f_{M-1} r_k - f_0 (M-1) d\sin\theta_k}{c_0}\right\} \end{bmatrix} \tag{6}$$

The corresponding transmit steering vector $\mathbf{a}(t;r,\theta)$ is

$$\mathbf{a}(t;r,\theta) = \begin{bmatrix} \exp(j2\pi\Delta f_0 t)\exp\left\{-j2\pi\frac{\Delta f_0 r}{c_0}\right\} \\ \exp(j2\pi\Delta f_1 t)\exp\left\{-j2\pi\frac{\Delta f_1 r - f_0 d\sin\theta}{c_0}\right\} \\ \vdots \\ \exp(j2\pi\Delta f_{M-1} t)\exp\left\{-j2\pi\frac{\Delta f_{M-1} r - f_0 (M-1) d\sin\theta}{c_0}\right\} \end{bmatrix} \tag{7}$$

The transmit beampattern can then be represented by

$$P(t;r,\theta) = \left(\mathbf{w}\otimes\mathbf{w}^\dagger\right)^T \left(\mathbf{a}(t;r,\theta)\otimes\mathbf{a}(t;r,\theta)^\dagger\right) \tag{8}$$

where $\otimes$ and † denote the Hadamard product and conjugate operators, respectively.

To form a focusing beampattern at the desired position, we utilize the power difference between the sidelobe region $\{S_1, S_2, S_3, S_4\}$ and the main beam region K, as shown in Fig. 1, and formulate the beampattern synthesis as a constrained nonlinear programming problem. The radiation power in main beam region is

$$P_K(t;r_K,\theta_K) = \left(\mathbf{w}*\mathbf{w}^\dagger\right)^T \left(\mathbf{a}(t;r_K,\theta_K)*\mathbf{a}(t;r_K,\theta_K)^\dagger\right) \tag{9}$$

while the radiation power corresponding to sidelobe region is

$$\mathbf{P}_S(t;\mathbf{r}_S,\mathbf{\Theta}_S) = \begin{bmatrix} \left(\mathbf{w}*\mathbf{w}^\dagger\right)^T \left(\mathbf{a}(t;r_{S_1},\theta_{S_1})*\mathbf{a}(t;r_{S_1},\theta_{S_1})^\dagger\right) \\ \left(\mathbf{w}*\mathbf{w}^\dagger\right)^T \left(\mathbf{a}(t;r_{S_2},\theta_{S_2})*\mathbf{a}(t;r_{S_2},\theta_{S_2})^\dagger\right) \\ \vdots \\ \left(\mathbf{w}*\mathbf{w}^\dagger\right)^T \left(\mathbf{a}(t;r_{S_4},\theta_{S_4})*\mathbf{a}(t;r_{S_4},\theta_{S_4})^\dagger\right) \end{bmatrix} \tag{10}$$

with $\mathbf{r}_S = [r_{s_1}, r_{s_2}, \cdots, r_{s_4}]^T$ and $\mathbf{\Theta}_S = [\theta_{s_1}, \theta_{s_2}, \cdots, \theta_{s_4}]^T$.

Mathematically, the focusing beampattern synthesis can be recast as

$$\hat{\mathbf{\Delta f}} = \arg\max_{\mathbf{\Delta f}} \left\{P_K(t;r_K,\theta_K) - \|\mathbf{P}_S(t;\mathbf{r}_S,\mathbf{\Theta}_S)\|_1\right\} \tag{11}$$

where $\|\cdot\|_1$ denotes the 1-norm of a vector, and the constrained frequency offset vector is

$$\mathbf{\Delta f} = \begin{bmatrix} \Delta f_0 & \Delta f_1 & \cdots & \Delta f_{M-1} \end{bmatrix} \tag{12}$$

At this point, we can use MATLAB built-in constrained nonlinear optimization tool to calculate the objective function (11). The computation steps are listed in **Algorithm** 1.

Algorithm 1 FDA range-angle focusing beamforming synthesis algorithm.

Input: t, M, d, c, f_0, θ_K, r_K;
Output: $\mathbf{\Delta f}$

1: Initialize the frequency-offset vector $\mathbf{\Delta f}$ randomly between Δf_{min} and Δf_{max}.
2: Fix the time t to a certain moment, notice that $t \in [0, T]$;
3: Design constrained nonlinear optimization problem by taking the negative (11);
4: Calculate the minimum of constrained nonlinear optimization problem specified by
fmincon (func, $\mathbf{\Delta f}, A, 0, Aeq, 0, \Delta f_{min}, \Delta f_{max}$) with $A = [], Aeq = []$;
5: **return** $\mathbf{\Delta f}$;

III. Simulation Results and Discussions

In this section, we simulate the FDA beampattern with our optimized frequency offsets and compare with typical existing frequency offset schemes. Unless state otherwise, we assume the FDA with 16 uniformly-spaced and isotropic elements operating at the carrier frequency f_0 = 10GHz. The initial frequency offsets Δf_m are generated randomly with the constraint scope $\Delta f_{\min} = -30$kHz and $\Delta f_{\max} = 30$kHz. Assume the desired position is $(r_K, \theta_K) = (75\text{km}, 25^\text{o})$ and the observation area ranges from 50km to 100km, while the whole range-angle region is $\Omega = \{50\text{km} \le r \le 100\text{km}, -90^\text{o} \le \theta \le -90^\text{o}\}$, the main beam region is $K = \{70\text{km} \le r \le 80\text{km}, 20^\text{o} \le \theta \le 30^\text{o}\}$.

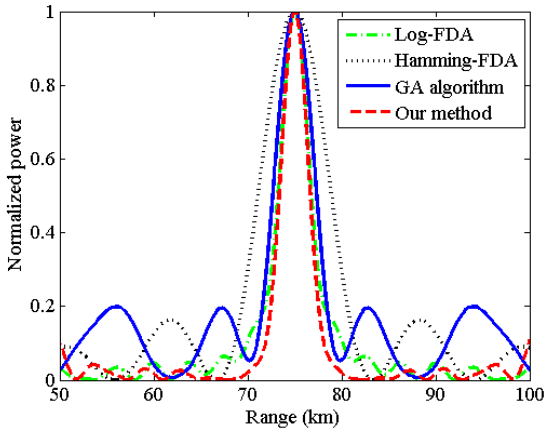

(a)

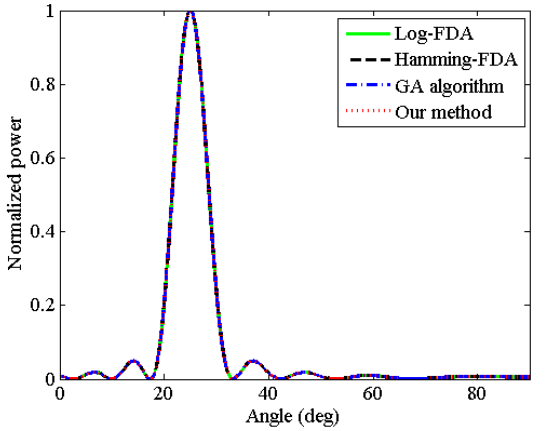

(b)

Fig. 2: 2-D FDA beampattern: (a) Range dimension; (b) Angle dimension.

TABLE I: COMPARISON OF THE FOCUSING PERFORMANCE

Method	$P(r,\theta)$		
	Spatial SLL	$HPBW_r$ [km]	$HPBW_\theta$ [deg]
Log-FDA	0.56	12.08	27.07
Hamming-FDA	0.39	7.88	7.27
GA-FDA	0.36	5.24	8.19
Our method	0.36	3.28	7.02

A. Focusing Beampattern Performance

Firstly, we compare the 2-D FDA beampattern (*i.e.* normalized power in range r and angle θ) at the observation time $t = 0$ between four schemes, namely, Log-FDA, Hamming-FDA, GA-FDA and our method, as shown in Fig. 2. Fig. 2(a) indicates that different frequency offsets generate distinct range-dimensional beampattern, which also shows that our method forms the narrowest main beam and the lowest sidelobe among four methods. Fig. 2(b) shows that the frequency offsets have no effects on the angle-dimension beampattern.

Secondly, Fig. 3 shows the 3-D FDA transmit beampattern,

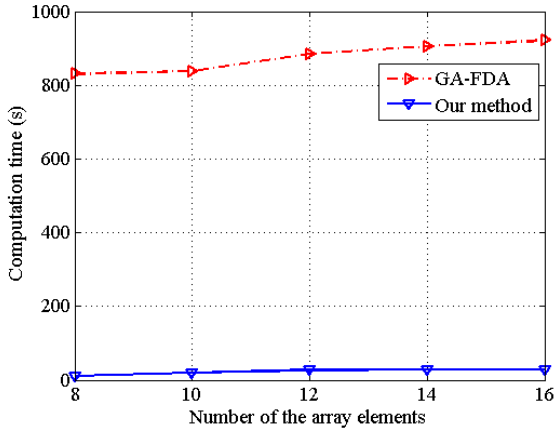

Fig. 4: Computation time with respect to number of the array elements.

where the beampatterm focusing effect is visually displayed. We can see that our method achieves the best focusing performance in both range and angle dimensions among four methods.

Finally, we evaluate the performance of four methods numerically in 3-D: Spatial sidelobe level (SLL), half-power beam width in the range dimension (HPBW_r) and angle dimension (HPBW_θ). Numerical results in Table I show that the spatial SLLs generated by GA-FDA and our method have lower sidelobe level with the same SLL = 0.36. In addition, the HPBW_r and HPBW_θ results obtained by our method are the best, which are 3.28 and 7.02, respectively.

It is noticed that our proposed method achieves similar focusing performance as GA-FDA. Further comparing simulations are carried out with a desktop computer equipped with 1 intel(R) core(TM) i5-6500 CPU at 3.2GHz and 8GB of RAM. The results given in Fig. 4 indicate that our method requires significant lower computation time than that for GA-FDA.

B. Time Variance Analysis and Discussions

To examine the FDA beampattern time variance, we simulate the FDA beampattern at two observation moments $t = \{0us, 30us\}$, as shown in the Fig. 5, which shows that the FDA focusing beampattern still is time variant and periodic, which is different from the conclusion in [21]–[23]. The main reason is that, the $\Delta f_m(t)$ in [21]–[23] is a function of time, but in fact $\Delta f_m(t)$ will change in with the signal propagation process, which is not consistent with the FDA actual transmitted signal.

IV. CONCLUSION

In this letter, we proposed a range-angle focusing FDA beampattern with nonuniform frequency offsets optimized by a constrained nonlinear programming. Numerical results show that the proposed method achieves superior focusing performance as well as low computational complexity, while compared with existing methods.

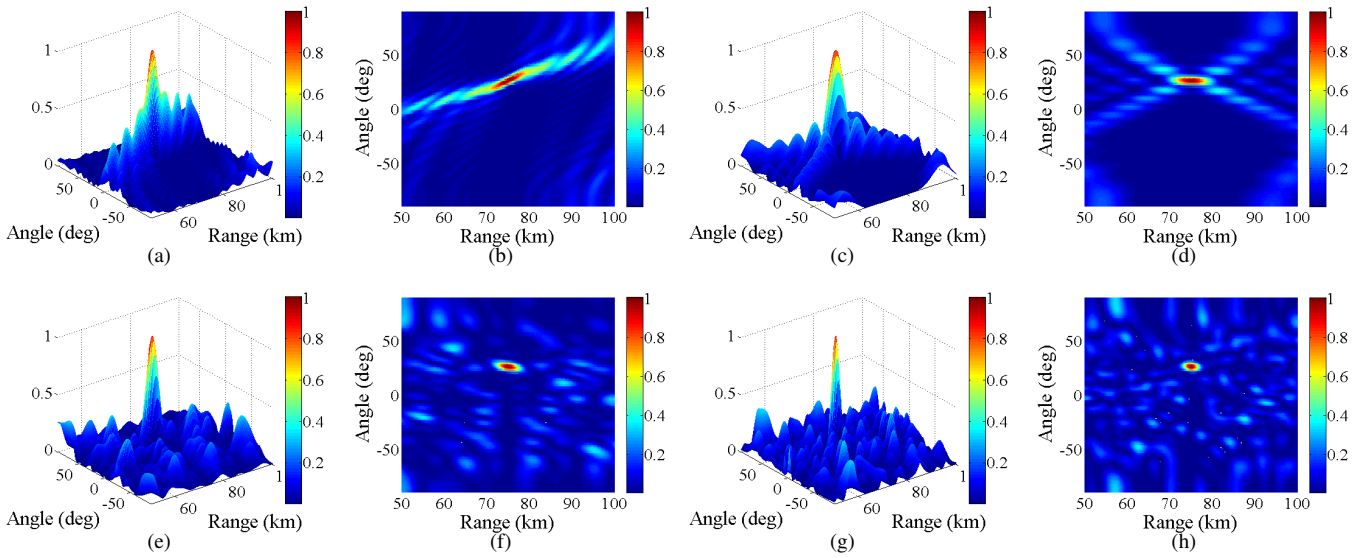

Fig. 3: FDA beampatterm ($t = 0$): (a)-(b) Log-FDA; (c)-(d) Hamming-FDA; (e)-(f) GA-FDA; (g)-(h) Our method.

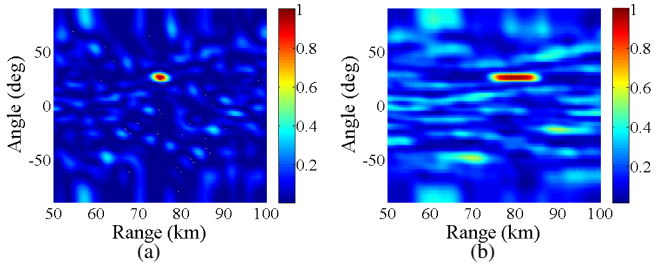

Fig. 5: FDA beampatterm considering time-variance ($T = 30us$): (a) $t = 0us$; (b) $t = 30us$

References

[1] W. Wang, "Frequency diverse array antenna: New opportunities," *IEEE Antennas and Propagation Magazine*, vol. 57, no. 2, pp. 145–152, April 2015.

[2] J. Xu, G. Liao, S. Zhu, L. Huang, and H. C. So, "Joint range and angle estimation using MIMO radar with frequency diverse array," *IEEE Transactions on Signal Processing*, vol. 63, no. 13, pp. 3396–3410, July 2015.

[3] P. Antonik, M. C. Wicks, H. D. Griffiths, and C. J. Baker, "Frequency diverse array radars," in *2006 IEEE Conference on Radar*, April 2006, pp. 3 pp.215–217.

[4] ——, "Multi-mission multi-mode waveform diversity," in *2006 IEEE Conference on Radar*, April 2006, pp. 3 pp.580–582.

[5] M. Secmen, S. Demir, A. Hizal, and T. Eker, "Frequency diverse array antenna with periodic time modulated pattern in range and angle," in *2007 IEEE Radar Conference*, April 2007, pp. 427–430.

[6] T. Higgins and S. D. Blunt, "Analysis of range-angle coupled beamforming with frequency-diverse chirps," in *2009 International Waveform Diversity and Design Conference*, Feb 2009, pp. 140–144.

[7] J. Shin, J. Choi, J. Kim, J. Yang, W. Lee, J. So, and C. Cheon, "Full-wave simulation of frequency diverse array antenna using the fdtd method," in *2013 Asia-Pacific Microwave Conference Proceedings (APMC)*, Nov 2013, pp. 1070–1072.

[8] W. Wang and H. Shao, "Range-angle localization of targets by a double-pulse frequency diverse array radar," *IEEE Journal of Selected Topics in Signal Processing*, vol. 8, no. 1, pp. 106–114, Feb 2014.

[9] W. Wang, "Subarray-based frequency diverse array radar for target range-angle estimation," *IEEE Transactions on Aerospace and Electronic Systems*, vol. 50, no. 4, pp. 3057–3067, October 2014.

[10] J. Farooq, M. A. Temple, and M. A. Saville, "Application of frequency diverse arrays to synthetic aperture radar imaging," in *2007 International Conference on Electromagnetics in Advanced Applications*, Sep. 2007, pp. 447–449.

[11] ——, "Exploiting frequency diverse array processing to improve SAR image resolution," in *2008 IEEE Radar Conference*, May 2008, pp. 1–5.

[12] J. Farooq, "Frequency diversity for improving synthetic aperture radar imaging," *Dissertations and Theses - Gradworks*, 2009.

[13] W. Wang, "Adaptive RF stealth beamforming for frequency diverse array radar," in *2015 23rd European Signal Processing Conference (EUSIPCO)*, Aug 2015, pp. 1158–1161.

[14] A. Basit, I. M. Qureshi, W. Khan, S. u. Rehman, and M. M. Khan, "Beam pattern synthesis for an FDA radar with hamming window-based nonuniform frequency offset," *IEEE Antennas and Wireless Propagation Letters*, vol. 16, pp. 2283–2286, 2017.

[15] Y. Wang, W. Wang, H. Chen, and H. Shao, "Optimal frequency diverse subarray design with Cramr-Rao lower bound minimization," *IEEE Antennas and Wireless Propagation Letters*, vol. 14, pp. 1188–1191, 2015.

[16] P. F. Sammartino, C. J. Baker, and H. D. Griffiths, "Frequency diverse MIMO techniques for radar," *IEEE Transactions on Aerospace and Electronic Systems*, vol. 49, no. 1, pp. 201–222, Jan 2013.

[17] J. Xiong and W. Wang, "Sparse reconstruction-based beampattern synthesis for multi-carrier frequency diverse array antenna," in *2017 IEEE International Conference on Acoustics, Speech and Signal Processing (ICASSP)*, March 2017, pp. 3395–3398.

[18] H. Shao, J. Dai, J. Xiong, H. Chen, and W. Wang, "Dot-shaped range-angle beampattern synthesis for frequency diverse array," *IEEE Antennas and Wireless Propagation Letters*, vol. 15, pp. 1703–1706, 2016.

[19] W. Khan, I. M. Qureshi, and S. Saeed, "Frequency diverse array radar with logarithmically increasing frequency offset," *IEEE Antennas and Wireless Propagation Letters*, vol. 14, pp. 499–502, 2015.

[20] J. Xiong, W. Wang, H. Shao, and H. Chen, "Frequency diverse array transmit beampattern optimization with genetic algorithm," *IEEE*

Antennas and Wireless Propagation Letters, vol. 16, pp. 469–472, 2017.

[21] A. Yao, W. Wu, and D. Fang, "Frequency diverse array antenna using time-modulated optimized frequency offset to obtain time-invariant spatial fine focusing beampattern," *IEEE Transactions on Antennas and Propagation*, vol. 64, no. 10, pp. 4434–4446, Oct 2016.

[22] ——, "Solutions of time-invariant spatial focusing for multi-targets using time modulated frequency diverse antenna arrays," *IEEE Transactions on Antennas and Propagation*, vol. 65, no. 2, pp. 552–566, Feb 2017.

[23] A. Yao, P. Rocca, W. Wu, A. Massa, and D. Fang, "Synthesis of time-modulated frequency diverse arrays for short-range multi-focusing," *IEEE Journal of Selected Topics in Signal Processing*, vol. 11, no. 2, pp. 282–294, March 2017.